chemosensors

MDPI

Article

"Out of Pocket" Protein Binding—A Dilemma of Epitope Imprinted Polymers Revealed for Human Hemoglobin

Xiaorong Zhang [1,†], Giorgio Caserta [2,†], Aysu Yarman [1], Eszter Supala [3], Armel F. Tadjoung Waffo [2], Ulla Wollenberger [1], Róbert E. Gyurcsányi [3,*], Ingo Zebger [2,*] and Frieder W. Scheller [1,*]

1 Institute of Biochemistry and Biology, University of Potsdam, Karl-Liebknecht Str. 24–25, 14476 Potsdam, Germany; zhang9@uni-potsdam.de (X.Z.); aysu.yarman@yahoo.de (A.Y.); uwollen@uni-potsdam.de (U.W.)
2 Institut für Chemie, PC 14 Technische Universität Berlin, Straße des 17. Juni 135, 10623 Berlin, Germany; giorgio.caserta@tu-berlin.de (G.C.); tadjoungwaffo@tu-berlin.de (A.F.T.W.)
3 BME "Lendület" Chemical Nanosensors Research Group, Department of Inorganic and Analytical Chemistry, Budapest University of Technology and Economics, Szt. Gellért tér 4, 1111 Budapest, Hungary; supalaeszter@edu.bme.hu
* Correspondence: robertgy@mail.bme.hu (R.E.G.); ingo.zebger@tu-berlin.de (I.Z.); fschell@uni-potsdam.de (F.W.S.)
† These authors contributed equally to this work.

Abstract: The epitope imprinting approach applies exposed peptides as templates to synthesize Molecularly Imprinted Polymers (MIPs) for the recognition of the parent protein. While generally the template protein binding to such MIPs is considered to occur via the epitope-shaped cavities, unspecific interactions of the analyte with non-imprinted polymer as well as the detection method used may add to the complexity and interpretation of the target rebinding. To get new insights on the effects governing the rebinding of analytes, we electrosynthesized two epitope-imprinted polymers using the N-terminal pentapeptide VHLTP-amide of human hemoglobin (HbA) as the template. MIPs were prepared either by single-step electrosynthesis of scopoletin/pentapeptide mixtures or electropolymerization was performed after chemisorption of the cysteine extended VHLTP peptide. Rebinding of the target peptide and the parent HbA protein to the MIP nanofilms was quantified by square wave voltammetry using a redox probe gating, surface enhanced infrared absorption spectroscopy, and atomic force microscopy. While binding of the pentapeptide shows large influence of the amino acid sequence, all three methods revealed strong non-specific binding of HbA to both polyscopoletin-based MIPs with even higher affinities than the target peptides.

Keywords: Molecularly Imprinted Polymers; epitope imprinting; non-specific binding; redox gating; SEIRA spectroelectrochemistry

Citation: Zhang, X.; Caserta, G.; Yarman, A.; Supala, E.; Waffo, A.F.T.; Wollenberger, U.; Gyurcsányi, R.E.; Zebger, I.; Scheller, F.W. "Out of Pocket" Protein Binding—A Dilemma of Epitope Imprinted Polymers Revealed for Human Hemoglobin. *Chemosensors* **2021**, *9*, 128. https://doi.org/10.3390/chemosensors9060128

Academic Editor: Barbara Palys

Received: 21 April 2021
Accepted: 31 May 2021
Published: 3 June 2021

1. Introduction

Hemoglobin (HbA) is a heme-containing tetrameric protein which acts in the reduced state as the oxygen carrier in blood [1]. It consists of two α and two ß subunits. Each subunit contains one non-covalently bound heme group as oxygen binding site [2]. The normal concentration of the tetrameric HbA in blood is 2.3 mM [3]. Determination of HbA in blood is one of the most frequently used analyses in the clinical laboratory. Decreased concentrations are indicative for anaemia [4]. Furthermore, traces of HbA in faeces are indicators of injuries of the colon, e.g., due to colon carcinomas [5]. The concentration of HbA and HbA1c in blood are routinely measured for the determination of the degree of glycated HbA—the long-term diabetic parameter [6]. Recently MIP based sensors which apply the whole spectrum of electrochemical and optical transducers made inroads in the determination of protein biomarkers [7–26] including SARS-COV-2 antigens [8]. For many years, Bülow's group made great efforts to create HbA-specific polymer beads for chromatographic separation of HbA variants from protein mixtures and crude cell

extracts [27–29]. The resulting chromatographic resins could be used to separate and purify HbA and fetal Hb from human body fluids and could identify changes in single amino acids on the Hb molecule surface [29]. Beside using the protein as the template, they also tried the epitope imprinting method to prepare Molecularly Imprinted Polymers (MIPs) [28]. This approach was initiated by Rachkov and Minoura [30,31]. They applied the N-terminal tripeptide of oxytocin as the template for a MIP for the whole nonapeptide. This concept has been successfully expanded to bio-macromolecular targets such as proteins. In these systems, 4 to 20 amino acid peptides are exploited for recognizing protein made up of several hundred amino acids (Table S1) [10,32–37].

Application of the epitope approach for the recognition of Hb is questionable because the N-termini of the ß-chains are located in the contact area of the protein subunits. To overcome this challenge, Bagan et al. [28] modified the epitope imprinting approach for the synthesis of a HbA-binding MIP. They introduced an intermediate step by generating the template for MIP-synthesis via hemoglobin immobilization to silica nanoparticles, through the N-terminal valines, followed by digestion of the protein using trypsin. This MIP-synthetic approach resulted only in a two-fold higher HbA binding as compared with the non-imprinted polymer (NIP) [9].

Whereas only a few papers presented MIPs for human HbA, bovine hemoglobin (BHb) has been frequently used as a "model protein" [38–47]. Reddy et al. synthesized a hydrogel-based imprinted polyacrylamide film deposited on a glassy carbon electrode for BHb detection. The successful synthetic approach was validated by recording the signal of electrochemical reduction of the heme-bound oxygen [48]. For the determination of HbA and HbA1c, the first MIP was described by Bossi et al. [49]. They polymerized aminophenyl boronic acid in the presence of the template proteins on polystyrene microplates. The HbA1c-MIP showed a three-times lower affinity towards HbA as compared with the target HbA1c.

Following the epitope approach, we have recently reported the successful synthesis of two types of peptide imprinted nanofilms for the recognition of the N-terminal HbA peptide and its glycated derivative HbA1c without assistance of boronate affinity [50]. MIP nanofilms were prepared either by a random, single-step electrosynthesis of scopoletin/pentapeptide mixtures or using a two-step hierarchical approach involving first a chemisorption of the cysteine extended N-terminal HbA pentapeptide followed by the electropolymerization of scopoletin [50]. The results revealed excellent discrimination of peptides differing in a single terminal fructosyl or a single amino acid unit.

Here, we resumed our previous investigation to target the rebinding of the entire HbA protein by using a corroborated square wave voltammetry (SWV), SEIRA spectroelectrochemistry, and atomic force microscopy (AFM) methodology. The results reveal major deviations from the simple binding model of the epitope imprinted polymer-parent protein that considers solely the interaction through the imprinted cavities.

2. Materials and Methods

2.1. Chemicals and Reagents

Scopoletin (7-hydroxy-6-methoxycoumarin) was purchased from Sigma Aldrich (Steinheim, Germany). Potassium hexacyanoferrate (III) (ferricyanide) and potassium hydroxide from Roth (Karlsruhe, Germany); potassium dihydrogen phosphate, potassium hexacyanoferrate (II) trihydrate (ferrocyanide) were obtained from Merck (Darmstadt, Germany); disodium phosphate from DuchefaBiochemie (Haarlem, The Netherlands); the proteins human Methemoglobin (MetHb) which contains Fe^{3+} in the heme, albumin from human serum (HSA), and albumin from bovine serum (BSA) were purchased from Sigma Aldrich (Steinheim, Germany). The peptides used in this study, i.e., the cysteine-extended N-terminus of ß-chain of HbA (cys-peptide or CVHLTP), the N-terminus of ß-chain of HbA (N-terminal peptide or VHLTP) were from Biosyntan GmbH (Berlin, Germany). All solutions were prepared using deionized water (DI water) obtained from a water purification system Milli-Q (Merck Chemicals GmbH, Darmstadt, Germany).

2.2. Electrochemical Measurements

Square wave voltammetry (SWV) was carried out in 1 mL of 5 mM ferri/ferrocyanide in phosphate buffered saline, pH 7.4 (PBS) containing 10 mM KCl with a CHI 440 electrochemical workstation (CH Instruments Inc., Austin, TX, USA) using a three-electrode electrochemical cell. Gold wires (diameter of 0.5 mm from Goodfellow, Germany) were used as working electrodes, a spiral platinum wire as the counter electrode and an Ag/AgCl as the reference electrode (RE-3V from ALS Co., Tokyo, Japan). The potential was scanned from −0.3 to +0.4 V at a frequency of 10 Hz, an amplitude of 50 mV and a step height of 3 mV. All measurements were carried out at room temperature.

2.3. MIP-Electrosynthesis, Template Removal, and Rebinding

The gold wire electrodes were cleaned in a boiling KOH solution (2.5 M) for 4 h followed by storage in concentrated H_2SO_4 overnight. Before usage, the electrodes were rinsed with DI water and kept in 65% HNO_3 for 10 min. After rinsing with DI water again, the electrodes were ready for use.

For the preparation of the peptide epitope imprinted nanofilms we followed the procedure described earlier [50]. The monomer/peptide mixture-based MIPs (random MIPs) were synthesized on the cleaned bare gold wire electrodes from a solution containing 0.5 mM scopoletin and 50 μM N-terminal peptide VHLTP-amide by applying 30 pulse cycles with each cycle consisting of a 0.0 and a +0.7 V pulse with a duration of 5 and 1 s, respectively. NIPs were prepared using the same procedure but omitting the peptide chemisorption on bare gold. For the two-step hierarchical imprinting process via a pre-immobilized peptide, the clean bare gold wire electrodes were first incubated in a PBS solution containing 50 μM cys-peptide for 5 min. The polyscopoletin layer was then formed by electropolymerization using a solution with 0.5 mM scopoletin, 10 mM NaCl, and 5% *v/v* ethanol and the same electrochemical pulse program used for the random MIP.

Electrochemical template removal (E-TR) for both types of MIPs was performed by polarizing the respective MIP nanofilm-modified electrodes in PBS at +900 mV for 30 s. After E-TR, the electrodes were rinsed for 5 min with DI water and dried gently under nitrogen stream. For rebinding experiments, the MIP-modified electrodes were placed in a stirred electrochemical cell, firstly filled with 1 mL of PBS solution containing 5 mM ferri/ferrocyanide, 10 mM KCl followed by sequential addition of 2 μL of the peptide or protein stock solution. SWV curves were recorded every 2 min (in a quiet solution) and a steady state was reached within 20 min. All electrochemical measurements were performed at room temperature.

2.4. SEIRA Spectroscopic Measurements

The same NIP and MIP films were prepared on nanostructured gold electrodes suitable for SEIRA spectroelectrochemical investigations. This in situ surface analytical technique allows the acquisition of IR spectra to detect changes occurring in the very close proximity to the gold surface (about 8 nm), which allows monitoring processes such as polymer synthesis, template removal [51]. A gold film was chemically deposited on a silicon prism suitable for ATR (attenuated total reflection) investigationsa and subsequently electrochemically cleaned resulting in an island-like nanostructure, as previously described [52]. The prism was then installed into a home-made spectroelectrochemical IR cell, mounted in an IFS66v/S FTIR spectrometer from Bruker equipped with a liquid nitrogen cooled MCT (Mercury-Cadmium-Telluride) detector. The gold film served as working electrode, whereby a Pt wire and an Ag/AgCl electrode were used as counter and reference electrodes, respectively. Spectra with 4 cm^{-1} resolution were recorded by averaging 400 scans. Binding assays were performed by dissolving the peptides in DI deionized water, yielding 5 mM stock solution, and then subsequent dilution in PBS to a final concentration of 50 μM. IR spectra were registered before, during, and after immobilization of the target peptide. A further spectrum was recorded after extensive rinsing with a buffer to confirm a stable binding of the template peptides. The buffer was then replaced with a scopoletin

solution (0.5 mM, 10 mM NaCl, 5% *v/v* ethanol) and the electrosynthesis of the MIP-was accomplished by applying 30 pulse cycles with each cycle consisting of 2 pulses of 0.0 V for 5 s and +0.7 V for 1 s. NIPs were prepared with the same workflow, but without template peptides. Electrochemical template removal from the gold surface and target rebinding were also followed by SEIRA spectroscopy.

2.5. Atomic Force Microscopy Measurements

NIP samples were prepared on silicon slides according to the previously detailed steps. The slides were covered with approximately 50 nm gold layer, which provided a highly smooth surface for the accurate thickness determination. The AFM measurements were carried out with Nanosurf FlexAFM (Switzerland) after electropolymerization, template removal and absorption of 1 µM HbA. For the investigations, Tap190Al-G cantilever (BudgetSensor) was used with a force constant of 48 N/m, a length of 225 µm and a tip radius less than 10 nm. To determine the thickness of the polymer film, first a topographic image was taken by scanning a 3 × 3 µm area in Tapping mode (300 points/line resolution, 88–91% set point, 400 mV free amplitude). Then, the film was removed on a 1 × 1 µm area in 3 consecutive cycles using Lateral Force mode (1 µN force, 200 points/line resolution). Subsequently, a new topographic image was taken over the scratched region in the tapping mode with the abovementioned parameters. Finally, the images were analyzed with Gwyddion software. The thickness of the polymer film was determined as the average difference between the polymer surface and the liberated gold layer.

3. Results and Discussion

3.1. Electrochemical Characterization of HbA Binding to the MIPs and Cross-Reactivity Studies

Quantitative information on rebinding of the glycated and the N-terminal peptides in scopoletin-derived MIP nanofilms were recently reported [50], revealing higher binding affinities and selectivity for a hierarchical MIP. These were attributed to the higher density and more homogenous orientation of the peptide template during polymerization. Therefore, we employed the same strategy for the rebinding of HbA molecule. Incubating the hierarchical MIP after electrochemical template removal (E-TR, +0.9 V vs. Ag/AgCl for 30 s) with solutions of different HbA concentrations exhibited a concentration-dependent decrease of the SWV peak current of the redox marker (Figure 1). This reflects a decreased permeation of the redox probe through the MIP films induced by HbA, which blocks/occupies the corresponding binding cavities.

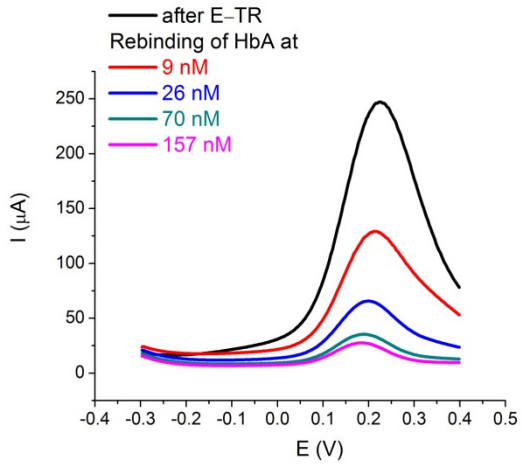

Figure 1. SWV responses of the hierarchical MIP recorded in a PBS solution at a pH of 7.4, containing 5 mM ferri/ferrocyanide and 10 mM KCl after electrochemical template removal (E-TR, black trace and after HbA rebinding using different protein concentrations (color code enclosed).

Notably, the observed current decrease detected for the binding of HbA was even larger than that of the template peptide (Figure 2). A K_d value of 9.06 ± 0.8 nM was obtained for HbA by using the Langmuir isotherm model, whereas a value of 64.6 ± 12.9 nM (Table 1) was determined for the peptide.

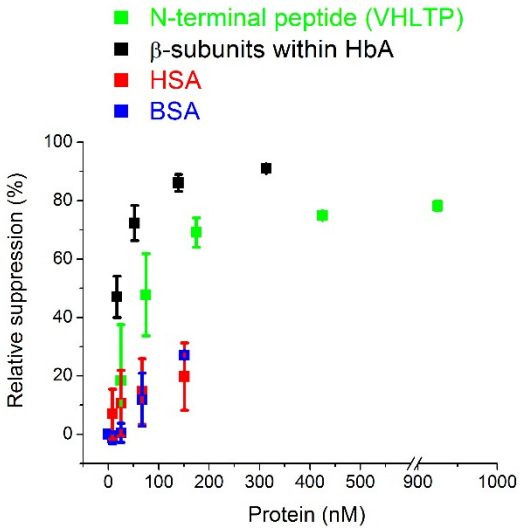

Figure 2. Comparison of the concentration-dependent relative suppression of the SWV signals (peak currents) detected for the binding of the template peptide VHLTP (green), HbA (concentration of ß-subunits of HbA, black), HSA (red), and BSA (blue) to the hierarchical MIP.

Table 1. K_d values determined for binding of the target peptide and HbA to the hierarchical and mixture-based MIPs.

MIP	Target	K_d
Hierarchical MIP (VHLTP template)	VHLTP	64.6 ± 12.9 nM [50]
	HbA	9.06 ± 0.8 nM
Random-MIP (VHLTP template)	VHLTP	1.4 ± 0.3 µM [50]
	HbA	20.4 ± 0.3 nM

The strong interaction with HbA was also observed for the random-MIP synthesized from a mixture of scopoletin and VHLTP peptide. While the random-MIPs showed more than a 20-fold lower affinity towards the target peptide (Table 1) than the hierarchical MIP, this difference decreases using the parent protein HbA. The comparably strong binding of HbA to both MIPs in combination with the weaker binding of the peptide to the random MIP results in values for the ratio of K_d for VHLTP and HbA of 7.13 for the hierarchical and 68.6 for the random MIP.

This difference arises presumably from the different synthetic approaches used in the two MIPs and is ascribed to less homogenous imprinting sites, where orientation effects might affect the binding affinity in the random approach. Nevertheless, the similar K_d values for HbA in both MIPs suggests a strong interaction of the protein with the polymer matrix. Indeed, it is reasonable that binding of HbA via its N-terminus can block the accessibility of several pores for the redox marker while the effect of target peptide is restricted to only one cavity.

Additionally, HbA possess an isoelectric point of 6.97, therefore, a change of the pH value from 7.4 to 5.2 leads to an inversion of the overall protein surface charge from a negative into a positive one. The polyscopoletin film on the other hand is negatively charged [33], in such way, the respective pH change of the reference solution (from pH 7.4 to pH 5.2) would transform a potential electrostatic interaction between polymer and HbA from a repulsive into an attracting one. However, rebinding assays performed at pH

5.2 resulted in decreased SWV responses for HbA at low concentrations and practically the same response at saturation concentrations (Figure 3), suggesting that electrostatic interactions do not play a major role in the HbA-MIP interaction.

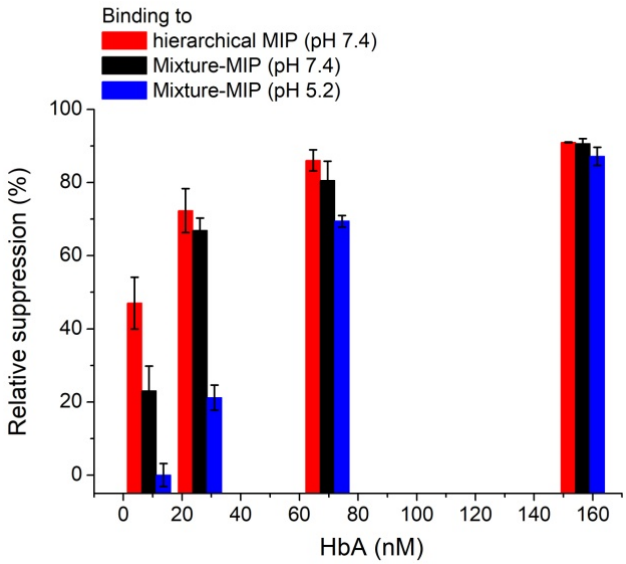

Figure 3. Comparison of the concentration-dependent relative suppression of the SWV signals (peak currents) detected for HbA rebinding to hierarchical MIP (red columns) and mixture-MIPs (black columns) in PBS buffer of pH 7.4, containing 5 mM ferri/ferrocyanide and 10 mM KCl. Measurements performed at pH 5.2 are indicated by blue columns.

Testing the cross-reactivity of the hierarchical MIP towards HSA and BSA (Figure 2), we observed that the SWV responses to the potential binding of both proteins was much lower compared to those for HbA and its N-terminal peptide. At the saturation level of HbA the response of the hierarchical MIP to these two proteins was four times lower, confirming a preferential binding of the target protein. Since it is unlikely that the pentapeptide specific epitopes are accessible to the much larger molecular weight BSA and HSA molecules, the most likely reason for the concentration dependent suppression of the current that is observed with these molecules is the out of pocket, non-specific binding on the non-imprinted surface of MIP nanofilm. However, because redox gating cannot verify the presence of HbA molecules on the polymer surface, we applied more informative SEIRA and AFM methodologies that target the direct polyscopoletin-HbA interaction.

3.2. SEIRA and AFM Characterization of HbA Binding to the NIP and Hierarchical MIP

As stated above, redox gating via SWV assays is an indirect method, which detects the electrochemical response of a redox probe accessing the underlying gold electrodes through the imprinted binding cavities. The target binding is detected through its concentration dependent blocking of these cavities, which gates the access of the redox probe. Consequently, the inherent binding of the proteins to the polymer scaffold by using NIPs cannot be investigated by this technique, i.e., NIPs films are insulating and due to the lack of imprinted cavities the redox marker access to the underlying electrode is fully suppressed and binding of the targets to the external surface cannot be detected. Therefore, in situ analysis such as SEIRA spectroelectrochemistry and subsequent AFM measurements was performed for further insight. These techniques were expected to additionally provide complementary structural information on the involved processes (e.g., nanofilms degradation, unspecific interaction of targets with the polymer scaffold). SEIRA spectroscopy has recently delivered key details in this respect. Thereby, the main advantage of using in situ spectroscopy is based on the possibility to record IR spectra of the individual steps of the MIP-synthesis performed on the gold film. Besides, we have also demonstrated the

fragility of scopoletin-derived nanofilms [50,53] to harsh chemical treatment, such NaOH exposure, which could eventually result in a degradation of the coumarin scaffold.

After chemisorption of CVHLTP-amide on bare gold electrode, we detected pronounced amide bands at 1674 and 1539 cm^{-1}, which remained constant in time. This results from a covalent immobilization of the peptide, possibly by Au-S/N bonds with His and Cys side groups (Figure 4, trace 1). Scopoletin electrosynthesis (Section 2.4) exhibited dominant IR absorptions at 1715 cm^{-1}, 1280 cm^{-1}, and 1235 cm^{-1}, indicative for the formation of a poly(alkyl ether) with a poly(ethylene oxide) backbone and coumarin side groups (Figure 4, trace 2) [50]. These bands partially superimpose the spectral contribution of the peptide target, which can be detected via a characteristic shoulder of the main absorption at 1715 cm^{-1}. The corresponding band is absent in NIP. Polymer bands are still detectable after electrochemical template removal, indicating no major changes in the polyscopoletin scaffold. The successive template removal is reflected by the disappearance of the shoulder bands at 1674 and 1539 cm^{-1}, which reappear after binding of HbA (Figure 4, trace 4, blue rectangles). In summary, the recorded SEIRA spectra allowed to monitor the entire hierarchical MIP forming process detecting the characteristic IR absorption bands for the polymer, peptide, and protein.

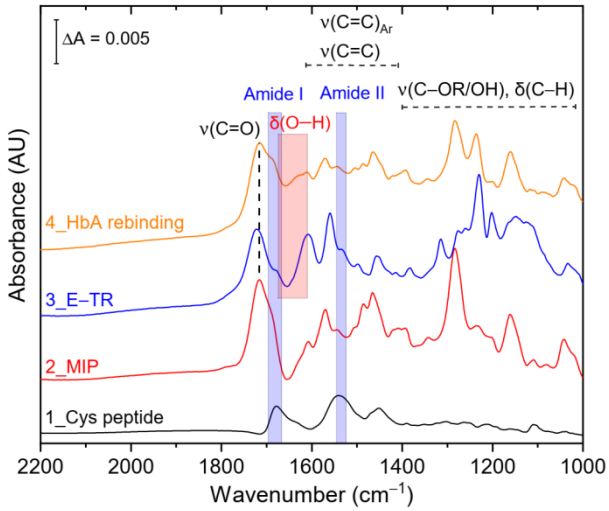

Figure 4. IR absorbance spectra of HbA binding to the hierarchical MIP on a SEIRA active gold electrode. Traces 1 to 3 display the individual steps of the MIP-formation. Trace 4 shows a rebinding using 500 µL of 1 µM HbA solution. HbA binding is confirmed by the detectability of amides I and II bands (blue rectangles). The red rectangle marks the broad O-H bending (δ) modes, centered at 1640 cm^{-1}, resulting from the permeability of the MIP film for water molecules via empty binding cavities [50].

As mentioned before, SEIRA spectroscopy involves the option to investigate protein/peptide interaction with non-imprinted nanofilms, where an electrochemical readout is not feasible due to the insulating properties of the NIPs nanofilms. Incubation of NIPs nanofilms with 0.1 µM HbA solution after different incubation times resulted in the spectral appearance of distinct amide I and amide II bands (Figure 5, left panel, blue rectangles) superimposing the specific polymer bands (Figure 5, trace 1). In such way, we revealed that HbA also binds strongly to the cavity-free NIP film. HbA remains bound on the NIP film despite extensive washing steps with high ionic strength buffer (PBS containing 1 M NaCl, Figure 5, left panel, trace 5). Washing HbA-bound NIP with NaOH solution, as recently reported, resulted in the polyscopoletin degradation (Figure 5, right panel, trace 3), while residual HbA was monitored by the respective amide I and amide II bands.

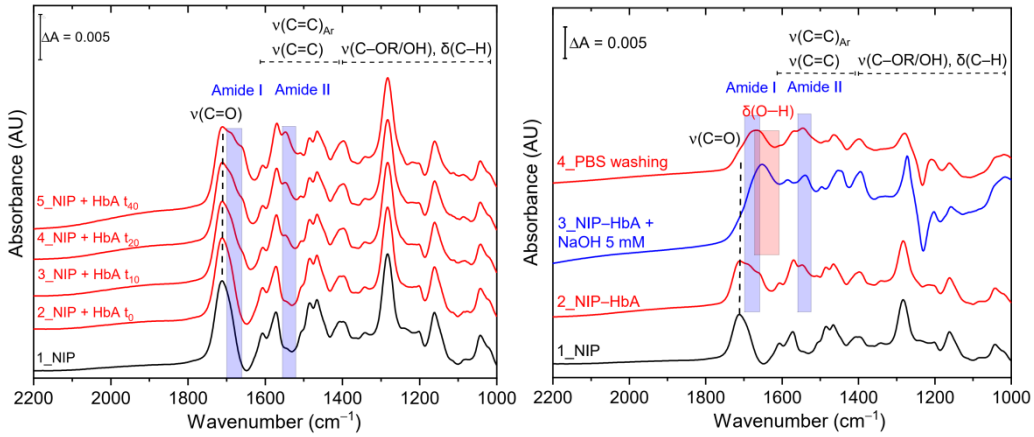

Figure 5. IR absorbance spectra of unspecific HbA binding on NIP. Spectra were recorded at different incubation times (left panel, 0, 10, 20, and 40 min) with 500 µL of PBS solution containing 0.1 µM HbA (pH 7.4). Note that after 40 min the electrode was washed with PBS containing 1 M NaCl resulting in no change of the amide I/II bands (trace 5). Washing with 5 mM NaOH (right hind panel, blue spectrum) resulted in NIP degradation, as derived from the disappearance of the absorption at 1715 cm^{-1}, while the HbA related amide II band at 1539 cm^{-1} band is still detectable (traces 3 and 4).

The binding of HbA on the polyscopoletin derived non-imprinted nanofilms was also confirmed by AFM-measurements (Table 2). While the +900 mV potential pulse did not have significant effect on the thickness of the nanofilm, it increased by almost 2 nm after the interaction with the protein sample (Figure S1).

Table 2. Average thickness of the non-imprinted polymer film determined by atomic force microscopy.

Sample	Thickness (nm)
After electropolymerization	9.3 ± 0.8
After anodic polarization	9.6 ± 0.1
After adsorption of 1 µM HbA	11.1 ± 0.5

In regard of the nature of the protein binding to the MIP and NIP film, we can largely rule out electrostatic interactions between HbA and the polyscopoletin matrix. Under the reported experimental conditions, with an adjusted pH value of 7.4, HbA harbors an overall negative charge, which would result in coulombic repulsions with the negatively charged polyscopoletin film [33]. The absence of electrostatic interactions is also supported by the observed lacking removal of NIP-bound HbA by exposure to 1 M NaCl solution in PBS (Figure 5, left panel, trace 5). This nonspecific binding was surprising, as polyscopoletin emerged so far as a rather resilient material to non-specific protein adsorption [54]. Altogether, these findings suggest that the HbA-polymer interplay relies prevalently on non-covalent, out-of-cavity hydrophobic interactions. This was confirmed by SEIRA spectroscopy, which reveals a significant removal of NIP-bound HbA protein by the non-ionic surfactant Tween as displayed in Figure 6. Indeed, the difference spectrum of "NIP-HbA + Tween" minus "NIP-HbA" (trace 3-2) revealed (i) negative amide I/II bands (Figure 6, blue rectangles) resulting from HbA removal and (ii) Tween binding on the polymer surface as highlighted by the symmetric CH_2 stretches at 2885 and 2994 cm^{-1}, respectively. Considering that Tween is generally used as detergent to remove unspecific hydrophobic interactions in biological assays, we corroborated the nature of the HbA-NIP interaction.

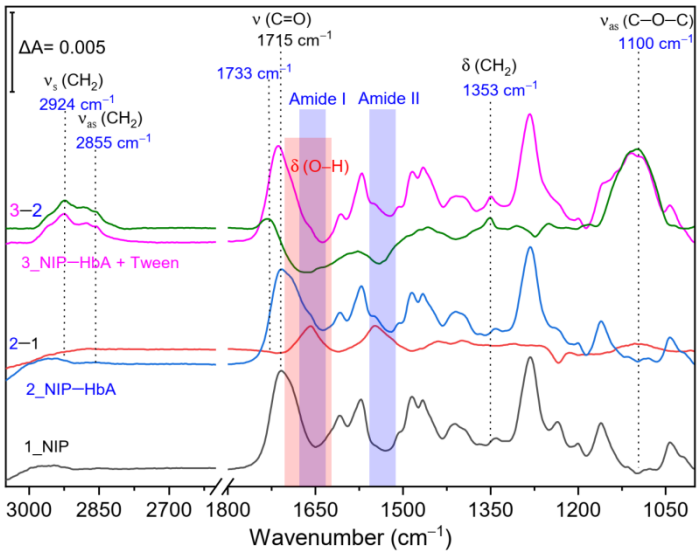

Figure 6. Effect of Tween on the HbA-NIP-nanofilm complex. The observed bands in trace 1 (dark) are attributed to the polyscopoletin NIP nanofilm. Trace 2 (blue) shows the unspecific HbA binding on the NIP, which is visualized in the corresponding difference spectrum between traces 2 and 1 (red spectrum). The related amides I and II absorptions are highlighted by the blue rectangle. Subsequent removal of HbA from the NIP film after addition of 0.05% Tween in PBS leads to spectral changes in amides I and II regions as depicted in trace 3 (magenta), these are displayed as negative absorptions bands in the respective difference spectrum between traces 3 and 2 (green trace). A concentration-dependent interaction of the surfactant with the polymer nanofilm is shown in the Supplementary Information (Figure S2).

4. Conclusions

In this study, we have observed that the binding of an entire protein to the epitope-imprinted MIPs can rely on the contribution of specific, cavity-related, and nonspecific, hydrophobic peptide/protein-polymer interactions. Blocking the non-imprinted polymer surface with proteins (as in immunoassays) would have interfered with the SEIRA measurements, i.e., the detection of hemoglobin would be masked by the IR signals related to the blocking protein as the amide bands appear in the same spectral range. For epitope-imprinted nanofilms a more sophisticated blocking procedure is needed with molecular level control.

Considering the original working hypothesis where a protein binds exclusively via its epitope functionality, the affinity towards the entire protein must not exceed the affinity for the epitope. Typically, target peptides in epitope-imprinted polymers have dissociation constants, K_d, in the nanomolar range while values in the micromolar range are observed for the corresponding proteins (Table S1). However, this holds only if the non-specific protein-polymer interactions are negligible. We demonstrated for our first epitope-MIP that the target peptide was stronger bound than the parent protein cytochrome c and competition between peptide and protein revealed the binding via the same cavities [33]. On the other hand, a K_d for the binding of the neurospecific enolase to the epitope MIP in the sub-nanomolar region was reported whereas the template peptide bound only in the μM-range [55]. In case of HbA, we have observed that hydrophobic protein-polymer interactions govern the protein rebinding, resulting in K_d lower than those reported for the peptide template. The nature and the strength of these non-specific interactions are plausibly dependent on the amino acid residues facing the protein surface. Obviously, the epitope approach has intrinsic limitations and future studies should be directed towards the exploitation of new protein-friendly and resilient polymer nanofilms hosting zwitterionic groups (e.g., polar for HbA protein rebinding), which might result in improved and ideally exclusive polymer/peptide specific interactions.

Supplementary Materials: The following are available online at https://www.mdpi.com/article/10.3390/chemosensors9060128/s1, Figure S1: (A) The topographic images of the non-imprinted polymer film were used for the thickness measurements after removal of a 1 × 1 µm rectangular area from the polymer. The removal stops at the underlying gold surface. The bright regions are due to removed material pushed to the sides of the rectangular area during the removal process. The difference of the film thickness (Δ) after and before adsorption of 1 µM HbA, as illustrated in the representative cross-sectional profiles (B), indicates the adsorption of HbA (see Table 2 for quantitative data), Figure S2: IR absorbance spectra of Tween binding on polyscopoletin (NIP), Table S1: MIPs prepared by epitope approaches. References [56–69] are cited in the Supplementary Materials.

Author Contributions: X.Z. and G.C. contributed equally to this work. Conceptualization, R.E.G. and F.W.S.; methodology, X.Z., G.C., A.Y., R.E.G. and I.Z.; formal analysis, X.Z., G.C., A.Y., E.S., A.F.T.W., R.E.G. and I.Z.; investigation, X.Z., G.C., E.S. and A.F.T.W.; writing—original draft preparation, X.Z., G.C., R.E.G. and F.W.S.; writing—review and editing, U.W., R.E.G., I.Z. and F.W.S.; visualization, X.Z., G.C., E.S., A.F.T.W. and R.E.G.; supervision, A.Y. and F.W.S.; project administration, F.W.S.; funding acquisition, U.W., R.E.G., I.Z. and F.W.S. All authors have read and agreed to the published version of the manuscript.

Funding: This research was funded by the Deutsche Forschungsgemeinschaft (D.F.G., German Research Foundation) under Germany's Excellence Strategy–EXC 2008–390540038–UniSysCat (to F.W.S., I.Z., U.W. and A.Y.). Further, G.C. and I.Z. are indebted for EU financial support (Article 38.1.2, GA) within the European Union's Horizon 2020 research and innovation program under grant agreement No 810856 and thank the Einstein Foundation Berlin (grant number EVF-2016-277) for additional funding. E.S. and R.E.G. gratefully acknowledge the BME Nanotechnology and Materials Science TKP2020 IE grant of NKFIH Hungary (BME IE-NATTKP2020) for financial support.

Conflicts of Interest: There are no conflict to declare.

References

1. Thom, C.S.; Dickson, C.F.; Gell, D.; Weiss, M.J. Hemoglobin Variants: Biochemical Properties and Clinical Correlates. *Cold Spring Harb. Perspect. Med.* **2013**, *3*, a011858. [CrossRef]
2. Yuan, Y.; Tam, M.F.; Simplaceanu, V.; Ho, C. New Look at Hemoglobin Allostery. *Chem. Rev.* **2015**, *115*, 1702–1724. [CrossRef]
3. Billett, H.H. *Chapter 151. Hemoglobin and Hematocrit*, 3rd ed.; Walker, H.K., Hall, W.D., Hurst, J.W., Eds.; Butterworths: Boston, MA, USA, 1990; ISBN 040990077X.
4. World Health Organization. *Haemoglobin Concentrations for the Diagnosis of Anaemia and Assessment of Severity*; WHO: Geneva, Switzerland, 2011.
5. Janz, T.; Lu, K.; Povlow, M.R.; Urso, B. A Review of Colorectal Cancer Detection Modalities, Stool DNA, and Fecal Immunochemistry Testing in Adults Over the Age of 50. *Cureus* **2016**, *8*, 931. [CrossRef]
6. Lyons, T.J.; Basu, A. Biomarkers in diabetes: Hemoglobin A1c, vascular and tissue markers. *Transl. Res.* **2012**, *159*, 303–312. [CrossRef] [PubMed]
7. Jetzschmann, K.J.; Zhang, X.; Yarman, A.; Wollenberger, U.; Scheller, F.W. Label-Free MIP Sensors for Protein Biomarkers. In *Label-Free Biosensing*; Springer: Berlin/Heidelberg, Germany, 2017; pp. 291–321.
8. Raziq, A.; Kidakova, A.; Boroznjak, R.; Reut, J.; Öpik, A.; Syritski, V. Development of a portable MIP-based electrochemical sensor for detection of SARS-CoV-2 antigen. *Biosens. Bioelectron.* **2021**, *178*, 113029. [CrossRef] [PubMed]
9. Di Giulio, T.; Mazzotta, E.; Malitesta, C. Molecularly Imprinted Polyscopoletin for the Electrochemical Detection of the Chronic Disease Marker Lysozyme. *Biosensors* **2020**, *11*, 3. [CrossRef]
10. Lee, M.-H.; Thomas, J.L.; Su, Z.-L.; Yeh, W.-K.; Monzel, A.S.; Bolognin, S.; Schwamborn, J.C.; Yang, C.-H.; Lin, H.-Y. Epitope imprinting of alpha-synuclein for sensing in Parkinson's brain organoid culture medium. *Biosens. Bioelectron.* **2021**, *175*, 112852. [CrossRef]
11. Wang, L.; Ma, Y.; Wang, L. High selectivity sensing of bovine serum albumin: The combination of glass nanopore and molecularly imprinted technology. *Biosens. Bioelectron.* **2021**, *178*, 113056. [CrossRef] [PubMed]
12. Gonçalves, L.M. Electropolymerized molecularly imprinted polymers: Perceptions based on recent literature for soon-to-be world-class scientists. *Curr. Opin. Electrochem.* **2021**, *25*, 100640. [CrossRef]
13. Cheubong, C.; Takano, E.; Kitayama, Y.; Sunayama, H.; Minamoto, K.; Takeuchi, R.; Furutani, S.; Takeuchi, T. Molecularly imprinted polymer nanogel-based fluorescence sensing of pork contamination in halal meat extracts. *Biosens. Bioelectron.* **2021**, *172*, 112775. [CrossRef] [PubMed]
14. Kalecki, J.; Iskierko, Z.; Cieplak, M.; Sharma, P.S. Oriented Immobilization of Protein Templates: A New Trend in Surface Imprinting. *ACS Sens.* **2020**, *5*, 3710–3720. [CrossRef] [PubMed]
15. Ramanavicius, S.; Jagminas, A.; Ramanavicius, A. Advances in Molecularly Imprinted Polymers Based Affinity Sensors (Review). *Polymers* **2021**, *13*, 974. [CrossRef]

16. Khumsap, T.; Corpuz, A.; Nguyen, L.T. Epitope-imprinted polymers: Applications in protein recognition and separation. *RSC Adv.* **2021**, *11*, 11403–11414. [CrossRef]
17. Hayden, O.; Lieberzeit, P.A.; Blaas, D.; Dickert, F.L. Artificial Antibodies for Bioanalyte Detection—Sensing Viruses and Proteins. *Adv. Funct. Mater.* **2006**, *16*, 1269–1278. [CrossRef]
18. Schirhagl, R.; Podlipna, D.; Lieberzeit, P.A.; Dickert, F.L. Comparing biomimetic and biological receptors for insulin sensing. *Chem. Commun.* **2010**, *46*, 3128–3130. [CrossRef]
19. Chunta, S.; Suedee, R.; Boonsriwong, W.; Lieberzeit, P.A. Biomimetic sensors targeting oxidized-low-density lipoprotein with molecularly imprinted polymers. *Anal. Chim. Acta* **2020**, *1116*, 27–35. [CrossRef]
20. Haupt, K.; Rangel, P.X.M.; Bui, B.T.S. Molecularly Imprinted Polymers: Antibody Mimics for Bioimaging and Therapy. *Chem. Rev.* **2020**, *120*, 9554–9582. [CrossRef] [PubMed]
21. Cruz, A.G.; Haq, I.; Cowen, T.; Di Masi, S.; Trivedi, S.; Alanazi, K.; Piletska, E.; Mujahid, A.; Piletsky, S.A. Design and fabrication of a smart sensor using in silico epitope mapping and electro-responsive imprinted polymer nanoparticles for determination of insulin levels in human plasma. *Biosens. Bioelectron.* **2020**, *169*, 112536. [CrossRef] [PubMed]
22. Moreira, F.T.; Ferreira, M.J.M.; Puga, J.R.; Sales, M.G.F. Screen-printed electrode produced by printed-circuit board technology. Application to cancer biomarker detection by means of plastic antibody as sensing material. *Sens. Actuators B Chem.* **2016**, *223*, 927–935. [CrossRef] [PubMed]
23. Ertürk, G.; Uzun, L.; Tümer, M.A.; Say, R.; Denizli, A. Fab fragments imprinted SPR biosensor for real-time human immunoglobulin G detection. *Biosens. Bioelectron.* **2011**, *28*, 97–104. [CrossRef]
24. Fresco-Cala, B.; Mizaikoff, B. Surrogate Imprinting Strategies: Molecular Imprints via Fragments and Dummies. *ACS Appl. Polym. Mater.* **2020**, *2*, 3714–3741. [CrossRef]
25. Moura, S.L.; Fajardo, L.M.; Cunha, L.D.A.; Sotomayor, M.D.P.T.; Machado, F.B.C.; Ferrão, L.F.A.; Pividori, M.I. Theoretical and experimental study for the biomimetic recognition of levothyroxine hormone on magnetic molecularly imprinted polymer. *Biosens. Bioelectron.* **2018**, *107*, 203–210. [CrossRef]
26. Sharma, P.S.; Iskierko, Z.; Noworyta, K.; Cieplak, M.; Borowicz, P.; Lisowski, W.; D'Souza, F.; Kutner, W. Synthesis and application of a "plastic antibody" in electrochemical microfluidic platform for oxytocin determination. *Biosens. Bioelectron.* **2018**, *100*, 251–258. [CrossRef]
27. Zhou, T.; Zhang, K.; Kamra, T.; Bülow, L.; Ye, L. Preparation of protein imprinted polymer beads by Pickering emulsion polymerization. *J. Mater. Chem. B* **2014**, *3*, 1254–1260. [CrossRef] [PubMed]
28. Bagán, H.; Zhou, T.; Eriksson, N.L.; Bülow, L.; Ye, L. Synthesis and characterization of epitope-imprinted polymers for purification of human hemoglobin. *RSC Adv.* **2017**, *7*, 41705–41712. [CrossRef]
29. Zhang, K.; Zhou, T.; Kettisen, K.; Ye, L.; Bülow, L. Chromatographic separation of hemoglobin variants using robust molecularly imprinted polymers. *Talanta* **2019**, *199*, 27–31. [CrossRef]
30. Rachkov, A.; Minoura, N. Towards molecularly imprinted polymers selective to peptides and proteins. The epitope approach. *Biochim. Biophys. Acta Protein Struct. Mol. Enzym.* **2001**, *1544*, 255–266. [CrossRef]
31. Rachkov, A.; Minoura, N. Recognition of oxytocin and oxytocin-related peptides in aqueous media using a molecularly imprinted polymer synthesized by the epitope approach. *J. Chromatogr. A* **2000**, *889*, 111–118. [CrossRef]
32. Yoshimatsu, K.; Yamazaki, T.; Hoshino, Y.; Rose, P.E.; Epstein, L.F.; Miranda, L.P.; Tagari, P.; Beierle, J.M.; Yonamine, Y.; Shea, K.J. Epitope Discovery for a Synthetic Polymer Nanoparticle: A New Strategy for Developing a Peptide Tag. *J. Am. Chem. Soc.* **2014**, *136*, 1194–1197. [CrossRef]
33. Dechtrirat, D.; Jetzschmann, K.J.; Stöcklein, W.F.M.; Scheller, F.W.; Gajovic-Eichelmann, N. Protein Rebinding to a Surface-Confined Imprint. *Adv. Funct. Mater.* **2012**, *22*, 5231–5237. [CrossRef]
34. Yang, K.; Li, S.; Liu, L.; Chen, Y.; Zhou, W.; Pei, J.; Liang, Z.; Zhang, L.; Zhang, Y. Epitope Imprinting Technology: Progress, Applications, and Perspectives toward Artificial Antibodies. *Adv. Mater.* **2019**, *31*, e1902048. [CrossRef]
35. Nishino, H.; Huang, C.-S.; Shea, K.J. Selective Protein Capture by Epitope Imprinting. *Angew. Chem. Int. Ed.* **2006**, *45*, 2392–2396. [CrossRef]
36. Singh, M.; Gupta, N.; Raghuwanshi, R. Epitope Imprinting Approach to Monitor Diseases. *J. Mol. Genet. Med.* **2017**, *11*, 1–6.
37. Iskierko, Z.; Sharma, P.S.; Noworyta, K.R.; Borowicz, P.; Cieplak, M.; Kutner, W.; Bossi, A.M. Selective PQQPFPQQ Gluten Epitope Chemical Sensor with a Molecularly Imprinted Polymer Recognition Unit and an Extended-Gate Field-Effect Transistor Transduction Unit. *Anal. Chem.* **2019**, *91*, 4537–4543. [CrossRef]
38. Xia, Y.-Q.; Guo, T.-Y.; Song, M.-D.; Zhang, B.-H.; Zhang, B.-L. Hemoglobin Recognition by Imprinting in Semi-Interpenetrating Polymer Network Hydrogel Based on Polyacrylamide and Chitosan. *Biomacromolecules* **2005**, *6*, 2601–2606. [CrossRef]
39. Gai, Q.; Liu, Q.; Li, W.; He, X.; Chen, L.; Zhang, Y. Preparation of bovine hemoglobin-imprinted polymer beads via the photografting surface-modified method. *Front. Chem. China* **2008**, *3*, 370–377. [CrossRef]
40. Kan, X.; Zhao, Q.; Shao, D.; Geng, Z.; Wang, Z.; Zhu, J.-J. Preparation and Recognition Properties of Bovine Hemoglobin Magnetic Molecularly Imprinted Polymers. *J. Phys. Chem. B* **2010**, *114*, 3999–4004. [CrossRef] [PubMed]
41. Li, D.-Y.; He, X.-W.; Chen, Y.; Li, W.-Y.; Zhang, Y.-K. Novel Hybrid Structure Silica/CdTe/Molecularly Imprinted Polymer: Synthesis, Specific Recognition, and Quantitative Fluorescence Detection of Bovine Hemoglobin. *ACS Appl. Mater. Interfaces* **2013**, *5*, 12609–12616. [CrossRef] [PubMed]

42. Zhou, T.; Ashley, J.; Feng, X.; Sun, Y. Detection of hemoglobin using hybrid molecularly imprinted polymers/carbon quantum dots-based nanobiosensor prepared from surfactant-free Pickering emulsion. *Talanta* **2018**, *190*, 443–449. [CrossRef] [PubMed]
43. Wu, S.; Tan, W.; Xu, H. Protein molecularly imprinted polyacrylamide membrane: For hemoglobin sensing. *Analyst* **2010**, *135*, 2523–2527. [CrossRef]
44. Kan, X.; Xing, Z.; Zhu, A.; Zhao, Z.; Xu, G.; Li, C.; Zhou, H. Molecularly imprinted polymers based electrochemical sensor for bovine hemoglobin recognition. *Sens. Actuators B Chem.* **2012**, *168*, 395–401. [CrossRef]
45. Li, L.; Yang, L.; Xing, Z.; Lu, X.; Kan, X. Surface molecularly imprinted polymers-based electrochemical sensor for bovine hemoglobin recognition. *Analyst* **2013**, *138*, 6962–6968. [CrossRef]
46. Wang, Z.; Li, F.; Xia, J.; Xia, L.; Zhang, F.; Bi, S.; Shi, G.; Xia, Y.; Liu, J.; Li, Y.; et al. An ionic liquid-modified graphene based molecular imprinting electrochemical sensor for sensitive detection of bovine hemoglobin. *Biosens. Bioelectron.* **2014**, *61*, 391–396. [CrossRef] [PubMed]
47. Li, Y.; Li, Y.; Hong, M.; Bin, Q.; Lin, Z.; Lin, Z.; Cai, Z.; Chen, G. Highly sensitive protein molecularly imprinted electro-chemical sensor based on gold microdendrites electrode and prussian blue mediatedamplification. *Biosens. Bioelectron.* **2013**, *42*, 612–617. [CrossRef]
48. Reddy, S.M.; Sette, G.; Phan, Q. Electrochemical probing of selective haemoglobin binding in hydrogel-based molecularly imprinted polymers. *Electrochim. Acta* **2011**, *56*, 9203–9208. [CrossRef]
49. Bossi, A.; Piletsky, S.A.; Piletska, E.V.; Righetti, P.G.; Turner, A.P.F. Surface-Grafted Molecularly Imprinted Polymers for Protein Recognition. *Anal. Chem.* **2001**, *73*, 5281–5286. [CrossRef] [PubMed]
50. Caserta, G.; Zhang, X.; Yarman, A.; Supala, E.; Wollenberger, U.; Gyurcsányi, R.E.; Zebger, I.; Scheller, F.W. Insights in electrosynthesis, target binding, and stability of peptide-imprinted polymer nanofilms. *Electrochim. Acta* **2021**, *381*, 138236. [CrossRef]
51. Osawa, M. Surface-Enhanced Infrared Absorption. In *Near-Field Optics and Surface Plasmon Polaritons*; Springer: Berlin/Heidelberg, Germany, 2001; pp. 163–187.
52. Miyake, H.; Ye, S.; Osawa, M. Electroless deposition of gold thin films on silicon for surface-enhanced infrared spectroelectrochemistry. *Electrochem. Commun.* **2002**, *4*, 973–977. [CrossRef]
53. Waffo, A.; Yesildag, C.; Caserta, G.; Katz, S.; Zebger, I.; Lensen, M.; Wollenberger, U.; Scheller, F.; Altintas, Z. Fully electrochemical MIP sensor for artemisinin. *Sens. Actuators B Chem.* **2018**, *275*, 163–173. [CrossRef]
54. Zhang, X.; Yarman, A.; Erdossy, J.; Katz, S.; Zebger, I.; Jetzschmann, K.J.; Altintas, Z.; Wollenberger, U.; Gyurcsányi, R.E.; Scheller, F.W. Electrosynthesized MIPs for transferrin: Plastibodies or nano-filters? *Biosens. Bioelectron.* **2018**, *105*, 29–35. [CrossRef]
55. Altintas, Z.; Takiden, A.; Utesch, T.; Mroginski, M.A.; Schmid, B.; Scheller, F.W.; Süssmuth, R.D. Integrated Approaches Toward High-Affinity Artificial Protein Binders Obtained via Computationally Simulated Epitopes for Protein Recognition. *Adv. Funct. Mater.* **2019**, *29*, 1807332. [CrossRef]
56. Warring, S.L.; Krasowska, M.; Beattie, D.A.; McQuillan, A.J. Adsorption of a Polyethoxylated Surfactant from Aqueous Solution to Silica Nanoparticle Films Studied with in Situ Attenuated Total Reflection Infrared Spectroscopy and Colloid Probe Atomic Force Microscopy. *Langmuir* **2018**, *34*, 13481–13490. [CrossRef]
57. Zhao, C.; Ma, X.; Li, J. An Insulin Molecularly Imprinted Electrochemical Sensor Based on Epitope Imprinting. *Chin. J. Anal. Chem.* **2017**, *45*, 1360–1366. [CrossRef]
58. Li, D.-Y.; Zhang, X.-M.; Yan, Y.-J.; He, X.-W.; Li, W.-Y.; Zhang, Y.-K. Thermo-sensitive imprinted polymer embedded carbon dots using epitope approach. *Biosens. Bioelectron.* **2016**, *79*, 187–192. [CrossRef] [PubMed]
59. Yang, K.; Liu, J.; Li, S.; Li, Q.; Wu, Q.; Zhou, Y.; Zhao, Q.; Deng, N.; Liang, Z.; Zhang, L.; et al. Epitope imprinted polyethersulfone beads by self-assembly for target protein capture from the plasma proteome. *Chem. Commun.* **2014**, *50*, 9521–9524. [CrossRef]
60. Yang, K.; Li, S.; Liu, J.; Liu, L.; Zhang, L.; Zhang, Y. Multiepitope Templates Imprinted Particles for the Simultaneous Capture of Various Target Proteins. *Anal. Chem.* **2016**, *88*, 5621–5625. [CrossRef] [PubMed]
61. Qin, Y.-P.; Jia, C.; He, X.-W.; Li, W.-Y.; Zhang, Y.-K. Thermosensitive Metal Chelation Dual-Template Epitope Imprinting Polymer Using Distillation–Precipitation Polymerization for Simultaneous Recognition of Human Serum Albumin and Transferrin. *ACS Appl. Mater. Interfaces* **2018**, *10*, 9060–9068. [CrossRef]
62. Moczko, E.; Guerreiro, A.; Cáceres, C.; Piletska, E.; Sellergren, B.; Piletsky, S.A. Epitope approach in molecular imprinting of antibodies. *J. Chromatogr. B Anal. Technol. Biomed. Life Sci.* **2019**, *1124*, 1–6. [CrossRef] [PubMed]
63. Ma, X.T.; He, X.W.; Li, W.Y.; Zhang, Y.K. Oriented surface epitope imprinted polymer-based quartz crystal microbalance sensor for cytochrome c. *Talanta* **2019**, *191*, 222–228. [CrossRef] [PubMed]
64. Xing, R.; Ma, Y.; Wang, Y.; Wen, Y.; Liu, Z. Specific recognition of proteins and peptides via controllable oriented surface imprinting of boronate affinity-anchored epitopes. *Chem. Sci.* **2019**, *10*, 1831–1835. [CrossRef] [PubMed]
65. Li, S.; Yang, K.; Liu, J.; Jiang, B.; Zhang, L.; Zhang, Y. Surface-Imprinted Nanoparticles Prepared with a His-Tag-Anchored Epitope as the Template. *Anal. Chem.* **2015**, *87*, 4617–4620. [CrossRef] [PubMed]
66. Li, S.; Yang, K.; Deng, N.; Min, Y.; Liu, L.; Zhang, L.; Zhang, Y. Thermoresponsive Epitope Surface-Imprinted Nanoparticles for Specific Capture and Release of Target Protein from Human Plasma. *ACS Appl. Mater. Interfaces* **2016**, *8*, 5747–5751. [CrossRef] [PubMed]
67. Li, S.; Yang, K.; Zhao, B.; Li, X.; Liu, L.; Chen, Y.; Zhang, L.; Zhang, Y. Epitope imprinting enhanced IMAC (EI-IMAC) for highly selective purification of His-tagged protein. *J. Mater. Chem. B* **2016**, *4*, 1960–1967. [CrossRef] [PubMed]

68. Ma, X.; Li, M.; Tong, P.; Zhao, C.; Li, J.; Xu, G. A strategy for construction of highly sensitive glycosyl imprinted electrochemical sensor based on sandwich-like multiple signal enhancement and determination of neural cell adhesion molecule. *Biosens. Bioelectron.* **2020**, *156*, 112150. [CrossRef]
69. Li, J.; Ma, X.; Li, M.; Zhang, Y. Does polysaccharide is an idea template selection for glycosyl imprinting? *Biosens. Bioelectron.* **2018**, *99*, 438–442. [CrossRef]